Fluid Phase Equilibria xxx (2016) 1–14

Contents lists available at ScienceDirect

Fluid Phase Equilibria

journal homepage: www.elsevier.com/locate/fluid

Direct detection of double retrograde behavior in binary systems for equation of state models

J.I. Ramello [a, b, c], J.M. Milanesio [b, c], G.O. Pisoni [a], M. Cismondi [b, c], M.S. Zabaloy [a, *]

[a] PLAPIQUI, Universidad Nacional del Sur, CONICET, CC 717, 8000, Bahía Blanca, Argentina
[b] IDTQ – Grupo Vinculado PLAPIQUI, CONICET, Argentina
[c] Facultad de Ciencias Exactas Físicas y Naturales, Universidad Nacional de Córdoba, Av. Vélez Sarsfield 1611, Ciudad Universitaria, X5016GCA, Córdoba, Argentina

ARTICLE INFO

Article history:
Received 16 December 2015
Received in revised form
24 February 2016
Accepted 26 February 2016
Available online xxx

Keywords:
Double retrograde behavior
Equation of state
Local extrema
Phase diagram

ABSTRACT

In this work, a straightforward methodology is proposed to establish at a glance, for binary systems, whether a model of the equation of state type predicts the occurrence of double retrograde behavior (DRB), and to also establish what the ranges of conditions of DRB existence are. This is accomplished by computing three hyper-lines, which usually are highly non linear. One of them is the vapor–liquid critical line. The other two are loci of cricondenbar points and of cricondentherm points. Each line is efficiently calculated in a single computer run by resorting to a robust numerical continuation method.

1. Introduction

A well-known and common phenomenon in the high pressure phase behavior of mixtures is the retrograde behavior (RB). RB was predicted by Van der Waals and, according to ref [1], observed experimentally for the first time by Kuenen (1897). Binary mixtures which are asymmetric, with respect to molecular size and/or shape and/or attractive forces, may present a more complex and less common phenomenon, i.e., the so-called double retrograde behavior (DRB). DRB usually occurs within a narrow range of composition, close to that of the pure lightest component.

Available data on DRB seem to be scarce. Examples of binary systems for which DRB was experimentally observed are the following: methane + n-butane [2], methane + n-pentane [3], NaCl + H_2O [4], ethane + limonene [5,6], ethane + linalool [7,8] and ethane + orange Peel oil [9] (pseudo-binary system). According to Alfradique and Castier [10], the scarcity of experimental information may be due to the fact that DRB occurs in very narrow composition ranges.

Deiters [11] and Raeissi and Peters [12], analyzed the DRB from a theoretical point of view, using the Gibbs–Konowalow equation, which is an extension of the Clayperon equation for multicomponent mixtures. Raeissi and Peters [6] described the DRB in the context of either isothermal or isoplethic (constant composition) phase equilibrium diagrams, i.e., they considered the DRB at constant temperature and composition. Different equations of state (EoS) were used to study the DRB [10,13,14]. EoSs are important models for describing the properties of vapor, liquid and supercritical phases. Unlike other models, EoS offer a continuous description of these three different states, as experimentally observed.

Raeissi and Peters [6] have studied the ranges of conditions of existence of the DRB using an EoS, by computing a number of phase equilibrium diagrams, for binary systems.

This approach, which is typical in the literature, is not straightforward, since several vapor–liquid equilibrium diagrams are to be computed to find the ranges of conditions within which the EoS predicts DRB. The availability of an alternative, more direct, approach for establishing the occurrence or absence of DRB is desirable. The goal of the present work was to propose and test one such alternative straightforward approach. This is accomplished by computing a couple of, in a way special, binary phase equilibrium diagrams, which make possible the direct determination of the ranges of conditions where liquid–vapor DRB occurs, for a given binary system, according to the EoS model chosen to describe its

* Corresponding author.
E-mail address: mzabaloy@plapiqui.edu.ar (M.S. Zabaloy).

http://dx.doi.org/10.1016/j.fluid.2016.02.044
0378-3812/

phase behavior.

One of the diagrams is named CCB diagram, and the other is named CCT diagram. The diagrams cover the whole mole fraction range, or only part of it, depending on the user's interest. A given diagram, out of the two DRB diagrams, is made of a couple of lines, each one calculated in a single computer run. One of the lines is always the binary critical line. The second line is either the CCB line or the CCT line. Different projections of these lines can be visualized to study the DRB phenomenon.

The cricondenbar (CCB, e.g., point 1 in Fig. 8) is the maximum pressure at which a mixture of given composition (isopleth) can be heterogeneous. Analogously, the cricondentherm (CCT, e.g., point 1 in Fig. 1) is the maximum temperature at which a mixture of given composition can be heterogeneous. For the detection of the DRB we have found that it is convenient to use an extended definition of the CCB and of the CCT. Thus, in this work, a CCB point is a stationary point (derivative equal to zero) of the vapor liquid-equilibrium pressure, and a CCT point is a stationary point of the vapor liquid-equilibrium temperature. Local maxima, local minima and inflection points are all stationary points.

A continuous set of binary isopleths has associated continuous sets of CCBs and of CCTs. Such binary CCB and CCT sets are respectively the CCB line and the CCT line (or hyperlines). They can be computed using an EoS. The analysis of the computed CCB and CCT diagrams lead either to detect the DRB or to discard its occurrence.

Wichterle [15] and Barrufet and Eubank [16] have shown that a CCB point is also a Cricondencomp at constant pressure (CCC_P).

A CCCp (e.g., point 1 in Fig. 9) is a phase equilibrium point, in a constant pressure diagram (Txy diagram), for which the mole fraction of one of the components (of the binary mixture) in one of the equilibrium phases is locally maximum. Notice that the (not shown) maximum temperature endpoint of the vapor–liquid region in Fig. 9 may be another critical point or a pure compound saturation point. This applies also to Figs. 12 and 14.

Similarly, a CCT point is also a Cricondencomp, but at constant temperature (CCC_T). More specifically, a CCC_T point (e.g., point 1 in Fig. 2) is a phase equilibrium point in a constant temperature diagram (Pxy diagram) for which the mole fraction of one of the components (of the binary mixture) in one of the equilibrium phases is locally maximum.

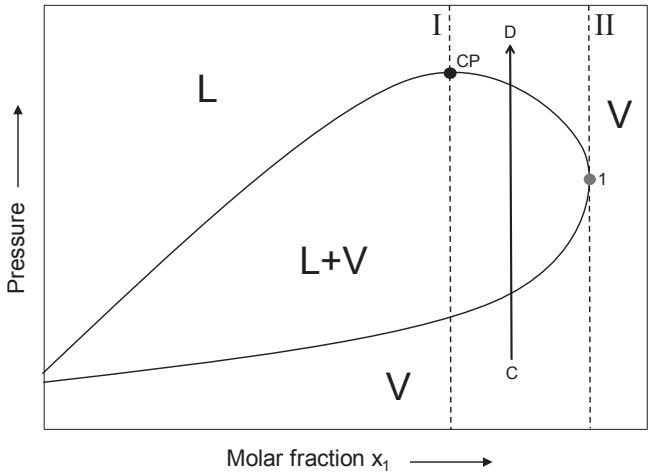

Fig. 2. Schematic Pressure-Molar fraction of component 1 diagram for a supercritical vapor–liquid equilibrium isotherm showing RBxT in the I–II composition range. CP: critical point. Point 1: CCC_T point.

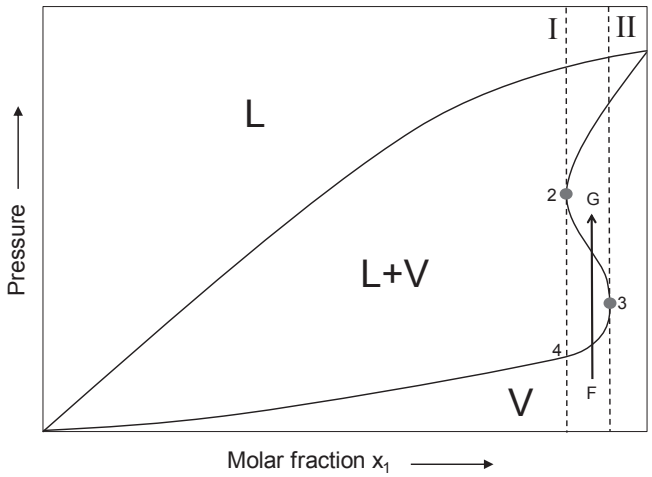

Fig. 3. Schematic Pressure-Molar fraction of component 1 diagram for a subcritical vapor–liquid equilibrium isotherm showing RBxT in the I–II composition range. Points 2 and 3: CCC_T points.

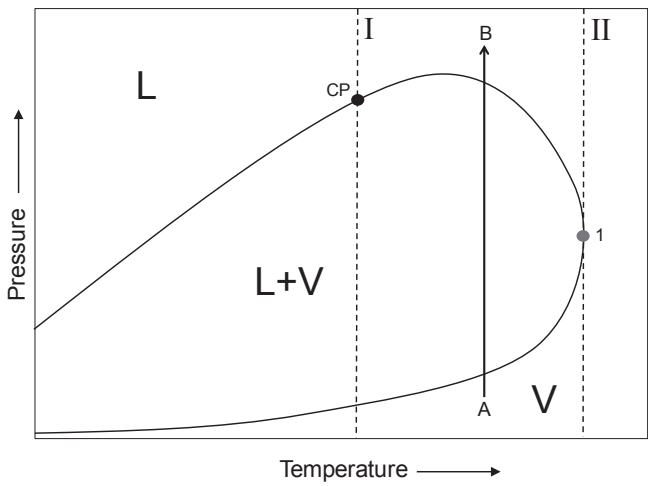

Fig. 1. Schematic Pressure–Temperature diagram for a vapor–liquid equilibrium isopleth showing RBxT in the I–II temperature range. CP: critical point. Point 1: CCT point.

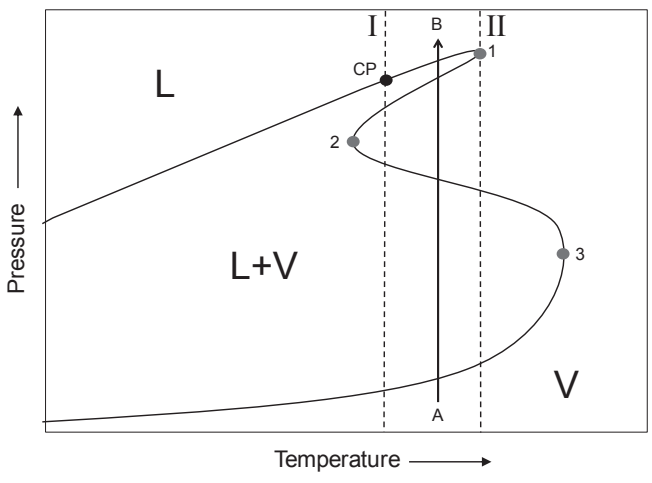

Fig. 4. Schematic Pressure–Temperature diagram for a vapor–liquid equilibrium isopleth showing DRBxT in the I–II temperature range. CP: critical point. Points 1, 2 and 3: CCT points.

Please cite this article in press as: J.I. Ramello, et al., Direct detection of double retrograde behavior in binary systems for equation of state models, Fluid Phase Equilibria (2016), http://dx.doi.org/10.1016/j.fluid.2016.02.044

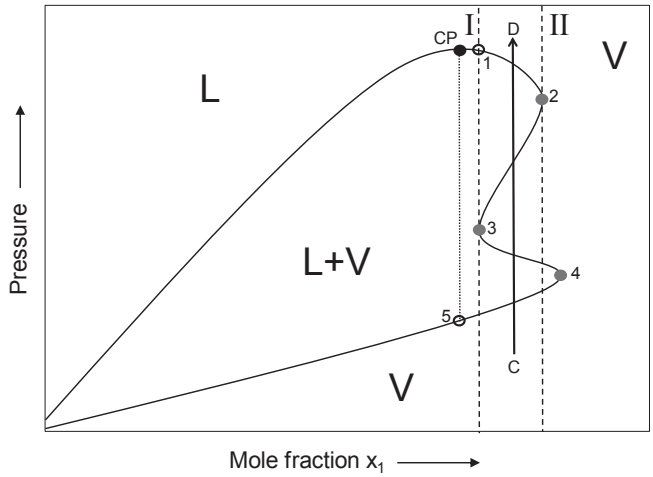

Fig. 5. Schematic Pressure-Molar fraction of component 1 diagram for a supercritical vapor–liquid equilibrium isotherm showing DRBxT in the I–II composition range. CP: critical point. Points 2, 3 and 4: CCC_T points.

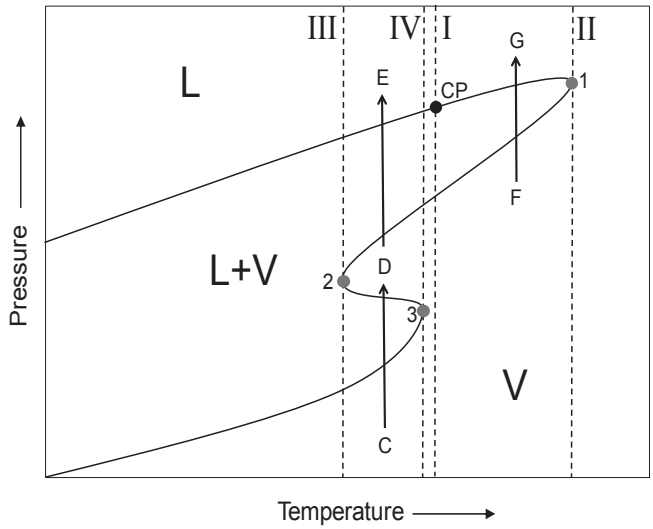

Fig. 6. Schematic Pressure–Temperature diagram for a vapor–liquid equilibrium isopleth showing RBxT in the I–II and III–IV temperature ranges. CP: critical point. Points 1, 2 and 3: CCT points.

Notice that the temperature, pressure, and phase compositions and densities, of a CCB point, are the same than those of its associated CCCp point. An analogous statement applies to a CCT point and its associated CCC_T point.

To fix ideas, it is important to make the following remarks:

- a CCB point is, simultaneously, a local extremum in pressure when the composition of one of the equilibrium phases is constant (isopleth), and a local extremum in the mole fraction of one of the components in one of the equilibrium phases at constant pressure (Isobaric Cricondencomp, CCC_P).
- a CCT point is, simultaneously, a local extremum in temperature when the composition of one of the equilibrium phases is constant (isopleth), and a local extremum in the mole fraction of one of the components in one of the equilibrium phases at constant temperature (Isothermal Cricondencomp, CCC_T).

Hence, a CCB line is also a CCC_P line, and a CCT line is also a CCC_T

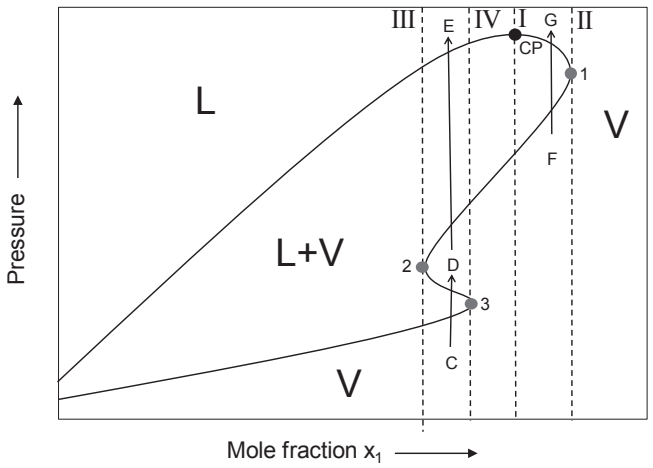

Fig. 7. Schematic Pressure-Mole fraction of component 1 diagram for a supercritical vapor–liquid equilibrium isotherm showing RBxT in the III–IV and I–II composition ranges. CP: critical point. Points 1, 2 and 3: CCC_T points.

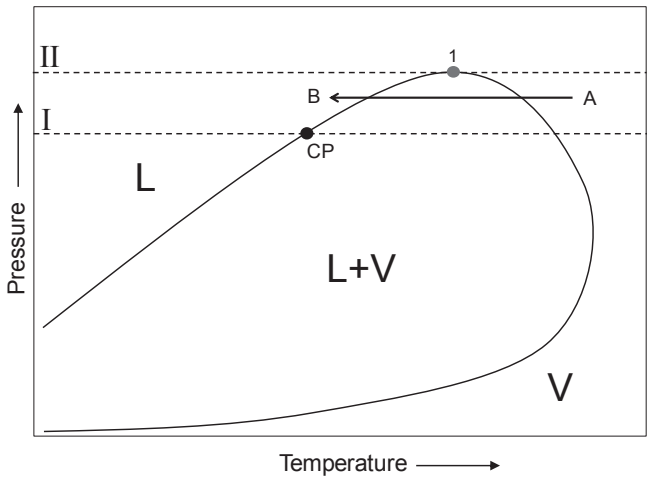

Fig. 8. Schematic Pressure–Temperature diagram for a vapor–liquid equilibrium isopleth showing RBxP in the I–II pressure range. CP: critical point. Point 1: CCB point.

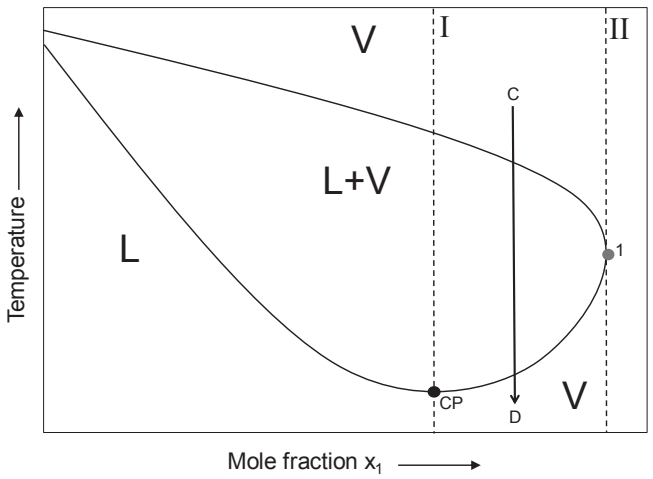

Fig. 9. Schematic Temperature-Mole fraction of component 1 diagram for a supercritical vapor–liquid equilibrium isobar showing RBxP in the I–II composition range. CP: critical point. Point 1: CCC_P point.

Please cite this article in press as: J.I. Ramello, et al., Direct detection of double retrograde behavior in binary systems for equation of state models, Fluid Phase Equilibria (2016), http://dx.doi.org/10.1016/j.fluid.2016.02.044

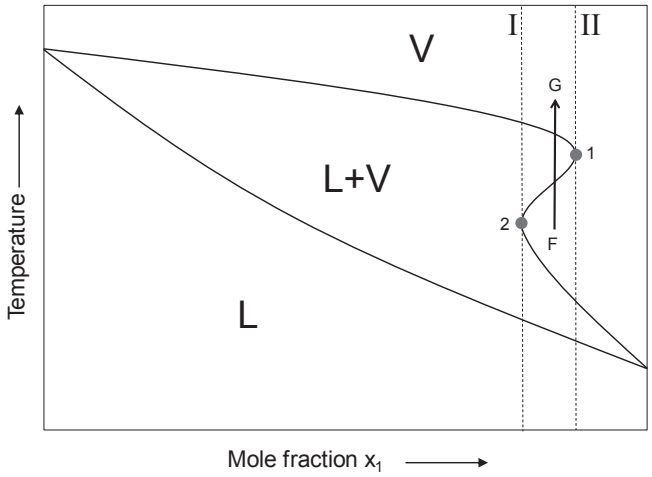

Fig. 10. Schematic Temperature-Mole fraction of component 1 diagram for a subcritical vapor–liquid equilibrium isobar showing RBxP in the I–II composition range. Points 1 and 2: CCC_P points.

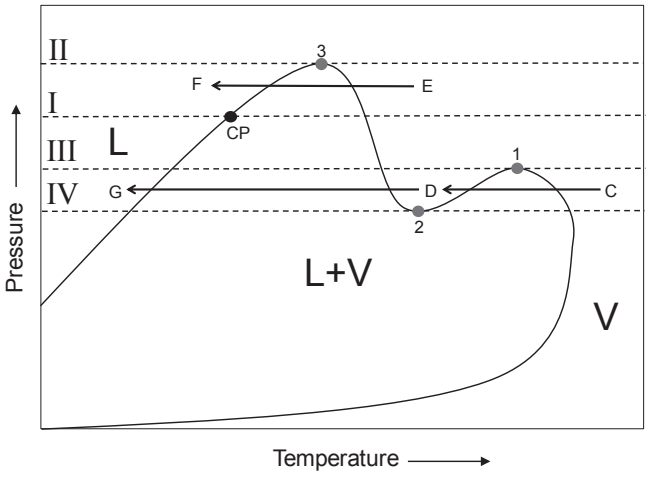

Fig. 13. Schematic Pressure–Temperature diagram for a vapor–liquid equilibrium isopleth showing RBxP in the I–II and IV–III pressure ranges. CP: critical point. Points 1, 2 and 3: CCB points.

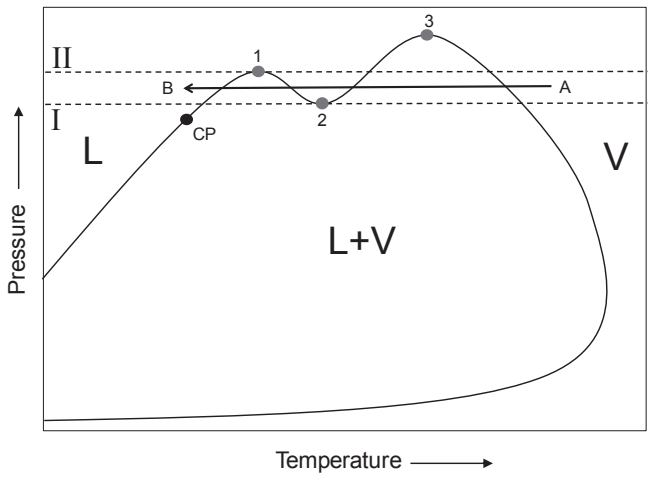

Fig. 11. Schematic Pressure–Temperature diagram for a vapor–liquid equilibrium isopleth showing DRBxP in the I–II pressure range. CP: critical point. Points 1, 2 and 3: CCB points.

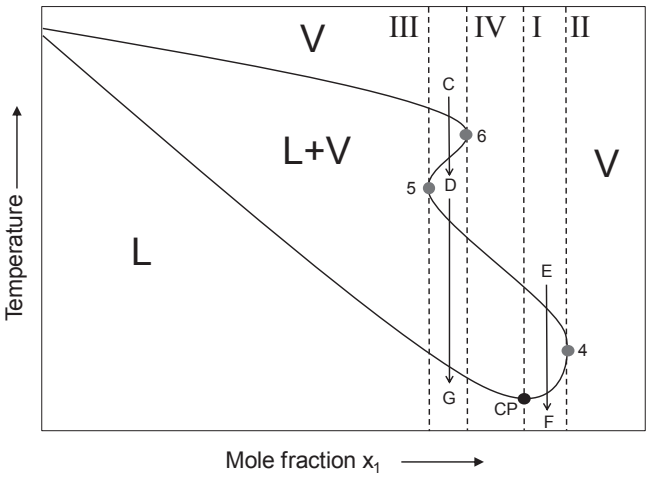

Fig. 14. Schematic Temperature-Mole fraction (x_1) diagram for a supercritical vapor–liquid equilibrium isobar showing RBxP in the III – IV and I–II x_1 ranges. CP: critical point. Points 4, 5 and 6: CCC_P points.

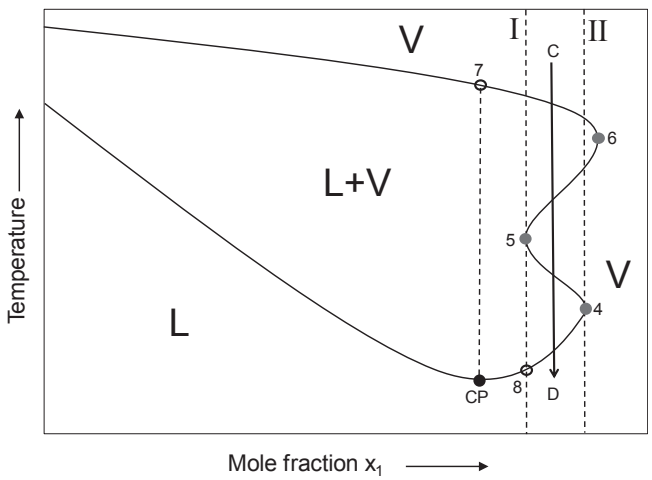

Fig. 12. Schematic Temperature-Mole fraction of component 1 diagram for a supercritical vapor–liquid equilibrium isobar showing DRBxP in the I–II composition range. CP: critical point. Points 4, 5 and 6: CCC_P points.

line. These lines may eventually contain a finite number of points which are inflection points to be seen in specific isothermal or isobaric or isoplethic phase equilibrium sections.

2. Variants for the retrograde behavior

In this section, we describe the variants found for the RB, on the basis of the present study and of some literature works [6,15,17].

Figs. 1–3 are schematic binary phase equilibrium diagrams showing retrograde behavior at constant composition and temperature (RBxT).

RBxT is present if two dew points are observed at set temperature and composition. This is shown in the isopleth of Fig. 1 (A–B trajectory). If the pressure is increased along the AB line (constant temperature) from point A to point B, then, the phase condition evolution is: Vapor (V) → Liquid (L) + Vapor (V) → Vapor (V). The retrograde stage of this evolution is the L + V → V stage. RB is observed in the temperature range enclosed by the vertical lines I and II.

If RBxT is observed at given temperature in a constant

composition section as the one of Fig. 1, then, it must also be observed at constant composition in the proper constant temperature section. This is illustrated in Fig. 2 (C–D trajectory) for a supercritical isotherm, and in Fig. 3 (F–G trajectory) for a subcritical isotherm (Pxy diagrams). By "supercritical isotherm" we mean that the temperature that defines the isotherm is in between the critical temperatures of the pure compounds; while "subcritical isotherm" means that such temperature is less than either of the two pure compound critical temperatures. Hence, a binary supercritical isotherm has a single pure-compound vapor–liquid equilibrium point, while a binary subcritical isotherm has two. The increasing pressure paths C–D in Fig. 2 and F–G in Fig. 3 have the sequence V→L + V→V. RB happens in the composition range enclosed by the vertical lines I and II both, in Figs. 2 and 3.

The double retrograde behavior at constant composition and temperature (DRBxT) is presented in Figs. 4 and 5. This behavior happens if four dew points are observed at set composition and temperature, as shown in the isopleth of Fig. 4, for the (increasing pressure) A-B path, and in the isotherm of Fig. 5, for the C-D path. In both cases, the evolution is V→L + V→V→L + V→V. Of this four steps the second and the fourth are the retrograde ones (L + V→V).

In Fig. 4, the DRBxT is found in between the vertical lines I and II, i.e., from the temperature of the critical point (CP) to the temperature of point 1, which is the local maximum in temperature of lowest temperature. In Fig. 5, DRBxT happens between the x_1 values of points 3 and 2.

Figs. 8–10 illustrate the case of retrograde behavior at constant composition and pressure (RBxP). Here, two dew points are observed as temperature decreases, as it is shown in Fig. 8 (isopleth, A-B path), Fig. 9 (supercritical isobar, C-D path) and Fig. 10 (subcritical isobar, G-F path). The progression as temperature decreases is V→L + V→V (retrograde stage: L + V→V).

The ranges for the RBxP are indicated by the lines I and II in Figs. 8–10. Notice that critical points, local maxima and local minima (e.g., Figs. 8–10) contribute to define the ranges of conditions of the RB and DRB. Such local extrema are for instance a CCB point (point 1 in Fig. 8), a CCC_P point (point 1 in Fig. 9), and a couple of CCC_P points in Fig. 10. The words "supercritical isobar" here mean that the isobar pressure is in between the pure compound critical pressures, while the words "subcritical isobar" mean that the pressure is less than either of them.

Finally, the double retrograde behavior at constant composition and pressure (DRBxP) takes place also when four dew points are observed (Fig. 11, isopleth, A-B path; and Fig. 12, isobar, C-D path). The observed progress again is V→L + V→V→L + V→V as temperature decreases. Notice in Fig. 11 that in the pressure range from P1 to P3 only RBxP is observed (not DRBxP), while the range of existence of DRBxP is set by the local extrema points 1 and 2. The retrograde transitions occur in Fig. 11 in part of the curve connecting points 2 and 3, and in part of the curve that connects point 1 and the critical point CP.

In Fig. 12, the range of existence of DRBxP is defined by points 5 and 4. The retrograde transitions are located in part of the curve connecting points 5 and 6, and in part of the curve connecting the CP and point 4.

This work deals with the RB related to the dew point line and not to the RB associated to the bubble point line. In this last case, the evolution L →L + V→ L is observed at constant pressure and composition, as temperature decreases (simple retrograde vaporization [upon temperature reduction]). If ever observed, the sequence for double retrograde vaporization associated to the bubble point line would be L → L + V→ L → L + V → L (upon temperature reduction at constant pressure and composition). This work does not deal either with what Kuenen named retrograde condensation of the second kind. This happens when the CCT temperature is located on the bubble point line (rather than on a dew point line) in an isopleth. At a temperature in between that of the CCT point and that of critical point, a liquid–vapor system would become a homogeneous liquid upon a pressure reduction.

3. Methodology

Through implicit differentiation it is possible to obtain the mathematical conditions valid at a CCB (and/or CCT) point. Such conditions are solved in a composition range by resorting to a numerical continuation method (NCM) to compute a full CCB (or CCT) locus. NCMs are the methods of choice for the straightforward computation of highly non-linear lines, which are made of points described by several coordinates (hyper-points). NCMs have been used extensively in the literature [18–23]. The mathematical CCB and CCT conditions considered in this work actually are the necessary condition of local extrema, i.e., of stationary points (not necessarily local maxima). In other words, the CCB and CCT conditions in this work encompass a wider range of situations than the conventional CCB and CCT definitions. From the calculation of these CCB (or CCT) hyper-lines, multiple local extrema in, e.g., a given isopleth can be detected. The presence of multiple local extrema in a given isopleth is characteristic of DRB.

More specifically, we start by writing the system of equations valid for a binary two-phase equilibrium, having a model of the equation of state (EoS) type in mind. The (fluid) phases are named phase "z" and phase "w". We first define the vector function $\overline{F}^{(4)}$ as follows:

$$\overline{F}^{(4)} = \begin{bmatrix} F_1 \\ F_2 \\ F_3 \\ F_4 \end{bmatrix} = \begin{bmatrix} P - h(T, z_1, v_z) \\ P - h(T, w_1, v_w) \\ \ln\widehat{f}_1(T, z_1, v_z) - \ln\widehat{f}_1(T, w_1, v_w) \\ \ln\widehat{f}_2(T, z_1, v_z) - \ln\widehat{f}_2(T, w_1, v_w) \end{bmatrix} \quad (1a.1 - 1a.4)$$

Next, we impose the equilibrium conditions, by setting $\overline{F}^{(4)}$ equal to the null vector:

$$\overline{F}^{(4)} = \begin{bmatrix} F_1 \\ F_2 \\ F_3 \\ F_4 \end{bmatrix} = \begin{bmatrix} P - h(T, z_1, v_z) \\ P - h(T, w_1, v_w) \\ \ln\widehat{f}_1(T, z_1, v_z) - \ln\widehat{f}_1(T, w_1, v_w) \\ \ln\widehat{f}_2(T, z_1, v_z) - \ln\widehat{f}_2(T, w_1, v_w) \end{bmatrix} = \begin{bmatrix} 0 \\ 0 \\ 0 \\ 0 \end{bmatrix} = \vec{0} \quad (1b.1 - 1b.4)$$

where P is the absolute pressure, T the absolute temperature, z_1 the mole fraction of component 1 in phase "z", w_1 the mole fraction of component 1 in phase "w", v_z the molar volume of phase "z" and v_w the molar volume of phase "w". Function "h" is the relationship between pressure, temperature, molar volume and composition set by the chosen EoS, considered to be explicit in pressure in Eq. (1b.1) and (1b.2). Such EoS determines the expression for the fugacity of component "i", i.e., $\widehat{f}_i$ [which appears in Eq. (1b.3) and (1b.4)], as a explicit function of temperature, molar volume and composition. Eq. (1b.1) and (1b.2) imply that the pressure is the same in both phases, and Eq (1b.3) and (1b.4) are the isofugacity conditions. The variables of the system of Eq (1b) are those of vector $\overline{X}_6$ which we define as follows:

$$\overline{X}_6^T = [T\ P\ z_1\ w_1\ v_z\ v_w] = [X_1\ X_2\ X_3\ X_4\ X_5\ X_6] \quad (2)$$

Since system (1b) has four equations and six variables, its number of degrees of freedom is two. Thus, system (1b) defines a binary two-phase equilibrium hyper-surface. The prefix "hyper" means in this work "existing in a space having more than three variables". A binary two-phase hyper-line becomes defined once

Please cite this article in press as: J.I. Ramello, et al., Direct detection of double retrograde behavior in binary systems for equation of state models, Fluid Phase Equilibria (2016), http://dx.doi.org/10.1016/j.fluid.2016.02.044

we make a specification that spends one of the two available degrees of freedom. Frequent specifications correspond to setting one of the variables of vector $\overline{X}_6$ equal to a constant. For instance the temperature T could be set as equal to 298.1 K. This would lead to an isothermal binary two-phase equilibrium hyper-line or diagram. Likewise, if a phase composition, e.g., w_1, is set equal to a constant value, then, a kind of isoplethic hyper-line or diagram would be obtained. Notice that this last choice only fixes the composition of one of the two equilibrium phases without specifying, for the heterogeneous system, the relative amount of such phase. Such relative amount is the so called phase mole fraction, which should not be confused with the mole fraction of a component in a given phase. Phase mole fractions are variables which have no influence on system 1b, i.e., they are not variables of system 1b.

At a CCB point (e.g., point 1 in Fig. 8), the derivative of pressure with respect to temperature, at constant composition for one of the phases at equilibrium, equals zero. This derivative is the derivative at a point of a curve (isopleth, e.g., Fig. 8) along which the equilibrium condition is preserved, i.e., along which system 1b remains satisfied. At a CCT point (e.g., point 1 in Fig. 1), the derivative of temperature with respect to the pressure equals zero. CBB and CCT points are points of the saturation curve (e.g., the curve in Fig. 1). Such curve is not explicitly defined as a function of the variable set as the independent one, but only implicitly, by system 1b.

To obtain the system of equations valid at a CCB point at a specified value for, e.g., w_1 , the following procedure is followed:

I. Obtain the expression for the total differential of functions F_1 to F_4 (which are defined in 1.a).
II. Set each of the previous differentials equal to zero (as required by system 1b).
III. Set the differential of the independent variable w_1 equal to zero (this is imposed by the “isopleth” condition).
IV. Divide the expressions obtained in item II by dT, i.e., by the differential of the remaining independent variable.
V. Set the ratio (dT/dT) equal to unity. This results in a subsystem of four equations whose variables are T, P, z_1, w_1, v_z *and* v_w and also the derivatives of P, z_1, v_z and v_w with respect to T, at set w_1. This system, together with system 1b, makes a system of 8 equations with 10 variables.

The new system is solved for the 8 variables that remain unknown after setting the desired value for w_1 ; and a zero value for the derivative $(dP/dT)_{\sigma,w_1}$ (CCB condition), where subscript “σ” means that the equilibrium condition is preserved in the differentiation process. For a range of w_1 values, the new system is solved and the values of the variables of interest (T, P, z_1, v_z *and* v_w) recorded. Thus, a locus of CCB points is generated, i.e., a CCB hyperline. This locus is computed in this work by using a numerical continuation method which is able to deal with the highly non-linear nature of CCB hyper-lines.

The procedure for obtaining the system of equations valid at a CCT point is analogous to the one described in items I to V. The key condition is in this case: $(dT/dP)_{\sigma,w_1} = 0$.

Notice that the system of 8 equations with 10 variables mentioned above becomes a system of 10 equations and 10 variables after setting the desired value for w_1; and a zero value for the derivative $(dP/dT)_{\sigma,w_1}$. In other words, the chosen value of w_1 does not need to be plugged into the equations where it appears. Otherwise, in our implementation, an equation that sets w_1 equal to a given value is added, thus increasing the number of equations from 8 to 9. Similarly, setting a zero value for $(dP/dT)_{\sigma,w_1}$ is done by adding the corresponding equation. In conclusion, we have a system of 10 equations with 10 unknowns, i.e., a “square” system. Such system includes a number of derivatives among its 10 variables. Technically, this system is a differential algebraic equation (DAE) system, because it is made of both, algebraic equations and differential equations (the latter are differential equations because a number of derivatives appear in their expressions). This might lead the reader to expect the application of a non elementary DAE solver, such as Runge-Kutta, in order to trace the CCB line. In this work, it was enough to apply Euler's method to predict the next point of the CCB line, after having available an already converged point. The procedure is essentially as follows: [a] set a value for w_1 (i.e., define one of the equations of the 10 × 10 system). [b] solve the 10 × 10 system (this provides a converged point of the CCB line, which includes all the values for the derivatives at such point). [c] Set a new value of w_1 by using a previously defined step size. [d] Using the known values for the derivatives at the converged point, predict, using Euler's method, the values of all variables of the CCB point at the new value of w_1. This is the predictor's result. [e] Use this result as an initialization of the 10 × 10 system, and solve it again. The result (corrector's result) is a new converged point of the CCB line. The algorithm that we have implemented is actually more sophisticated, since, before computing the next CCB point, the specified variable is not necessarily w_1. Otherwise, it is chosen automatically so that the problems associated to turning points are avoided. A turning point appears when, along the CCB hyper-line, a variable reaches a local maximum or a local minimum. The automatic choice of the specified variable was of utmost importance in this work, due to the highly non-linear nature of computed CCB and CCT lines. Besides, the step size in the specified variable is not made constant during the computation of CCB or CCT lines: its value is set on the basis of the convergence history of the last converged point. For more details on numerical continuation methods, the reader is referred to the specialized textbooks on the subject, and to previous papers of our group.

4. Results and discussion

In what follows we present, for a binary mixture, EoS based calculated critical lines and CCB and CCT loci, which make possible to establish whether the model predicts the occurrence of vapor—liquid DRB, and, in such a case, to identify the ranges of conditions of DRB existence. Each of the three lines is computed in a single run. In this way, the computation of several phase equilibrium isopleths and/or isotherms and/or isobars, for detection of the DRB, is avoided. All calculation results in this section are for the CO_2 + n-decane system and they were obtained using the RK-PR EoS coupled to mixing rules cubic with respect to mole fraction (CMRs) with parameters obtained from Cismondi et al. [24]. The behavior of this system, both experimentally and for the model, is of Type II in the Scott and van Konynenburg classification [25] (see Ref. [26] for more details on the classification of the fluid phase behavior).

4.1. Results on retrograde behavior at constant composition and pressure (RBxP, DRBxP)

Fig. 15 presents the computed CCB and CCT lines in their PT projections for system CO_2 + n-decane in the CO_2-rich region. To complete the diagram, the critical line and the carbon dioxide vapor pressure curve are also included. To fix ideas, a point belonging to the CCB line has the temperature and pressure coordinates at which some isopleth has a CCB point. A analogous statement is valid for a point of the CCT line. The saturated phase composition which defines an isopleth is not shown in Fig. 15. Notice that the “saturated phase composition” is the phase composition that remains constant in an isopleth. This composition may be that of the vapor phase (dew point) or that of the liquid phase (bubble point).

Although the system CO_2 + n-decane is of type II in the Scott and

Please cite this article in press as: J.I. Ramello, et al., Direct detection of double retrograde behavior in binary systems for equation of state models, Fluid Phase Equilibria (2016), http://dx.doi.org/10.1016/j.fluid.2016.02.044

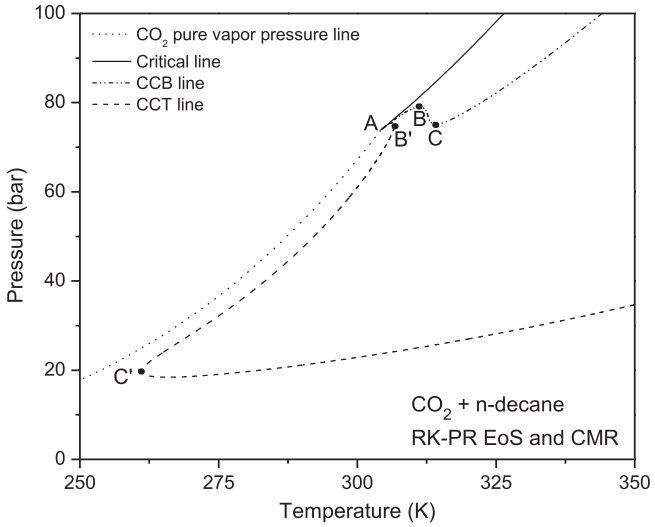

Fig. 15. CCB/CCT diagram. Calculated Pressure–Temperature projection of CCB and CCT lines in the CO_2-rich region. CO_2 + n-decane system (Type II in Scott and van Konynenburg classification [25,26]). Point A: CO_2 critical point. All lines were calculated using the RK-PR EoS and CMRs with parameters obtained from Cismondi et al. [24]. Points B and C: local maximum and local minimum in pressure of CCB line. Points B′ and C′: local maximum and local minimum in temperature of CCT line.

Van Konynenburg classification [25], RB and DRB are qualitatively identical to those observed in type I. This is because the liquid-liquid-vapor (LLV) line does not interfere with the CCT and CCB lines for this system.

Fig. 15 shows that the CCB line has a local maximum (point B) and a local minimum (point C) in pressure. The CCT line shows two local extrema in temperature (points B′ and C′).

4.1.1. Analysis of vapor–liquid equilibrium isopleths (RBxP, DRBxP)

Fig. 16 shows the CCB and critical lines in the CO_2-rich region, but in its Pressure- "saturated phase CO_2 mole fraction" projection. This projection provides the number (and pressure values) of CCB points for a given isopleth. Similarly, it provides the number (and composition values) of CCC_P points for a given isobar. Hence, this is the appropriate projection for establishing the eventual existence and types of RB associated to the CCB line.

In Fig. 16 the branches LMAX-1 and LMAX-2 are loci of isopleth local maxima in pressure, and the LMIN branch is the locus of isopleth local minima in pressure. Simultaneously, branches LMAX-1 and LMAX-2 are loci of isobar local maxima in saturated phase CO_2 mole fraction (xCO_2), and branch LMIN is a locus of isobar local minima in xCO_2. Notice that a local minimum (maximum) in xCO_2 must be a local maximum (minimum) in the saturated phase n-decane mole fraction (xC10).

In Fig. 16, the CCB line goes from point A (CO_2 critical point) to point B, next to point C, and extends to higher pressures and lower CO_2 mole fraction values. Point B is simultaneously a local maximum in pressure and a local minimum in the saturated phase CO_2 mole fraction of the CCB line. Point C is a local minimum in pressure and a local maximum in the saturated phase CO_2 mole fraction. Points B and C are cusps in the projection of Fig. 16, but they are not so in other projections, e.g., those in Figs. 15 and 20. Hence, points B and C are not cusps in the multi-dimensional space where the CCB line exists.

Fig. 18 shows a set of calculated vapor–liquid equilibrium isopleths together with the calculated CCB line previously presented in Fig. 15. It is seen that the CCB line connects the stationary points (derivative of pressure with respect to temperature at constant saturated phase composition equal to zero) of all isopleths. Clearly, some of the stationary points are local minima in pressure, some local maxima, and a couple of them are inflection points with zero slope (points B and C).

In Fig. 16, the isopleth with CO_2 mole fraction of 0.9965 (isopleth XII, vertical line) intersects the CCB projection at a single point, i.e., at point f (pressure about 82.5 bar). Point f is a maximum in pressure for isopleth XII (point f in Fig. 18). Isopleth XII (Figs. 16 and 18) shows RBxP. Any other point belonging to the LMAX-2 branch of the CCB line in Fig. 16, has the same character than point f, i.e., it is a (local or absolute) maximum in pressure for some isopleth (see in Fig. 18 the part of the CCB line that originates at point C and extends to higher temperatures, and see its intersection points, with the shown isopleths, e.g., points 15, 6, 1 in Fig. 18). As it is the case for

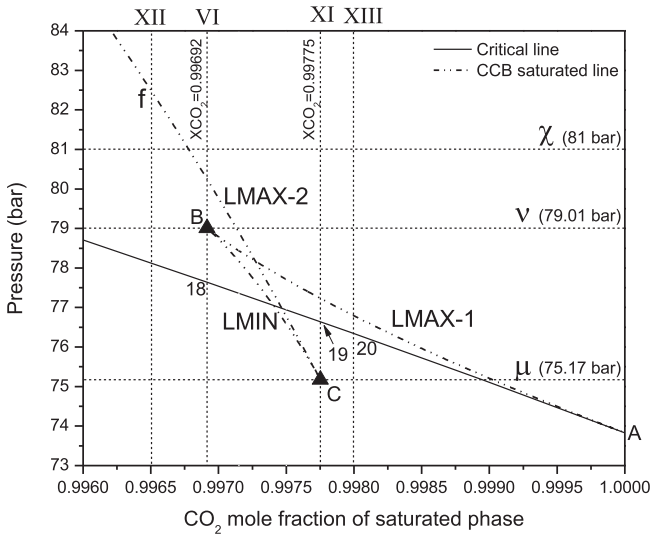

Fig. 16. CCB diagram. Pressure-CO_2 mole fraction in saturated phase projection of calculated CCB line. The calculated critical line is also shown. CO_2 + n-decane system. Horizontal dotted lines: constant pressure cuts. Vertical dotted lines: constant CO_2 mole fraction in saturated phase cuts. See caption of Fig. 15. Point B: local maximum in pressure and local minimum in CO_2 mole fraction in saturated phase. Point C: local minimum in pressure and local maximum in CO_2 mole fraction in saturated phase.

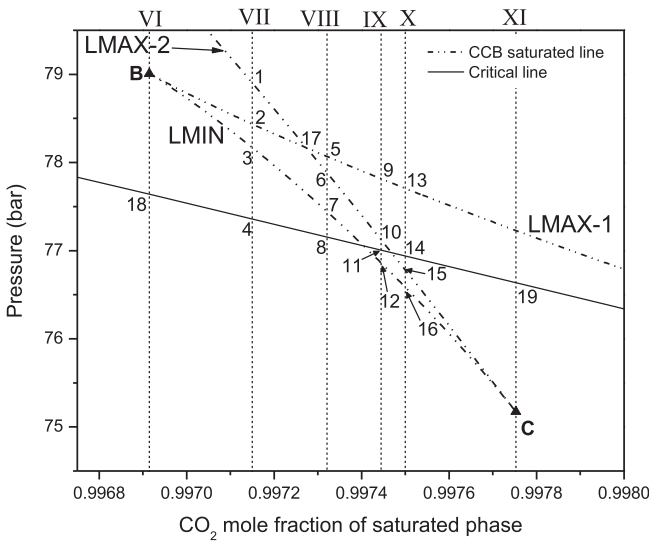

Fig. 17. Calculated CCB diagram. CO_2 + n-decane system. Vertical dotted lines: cuts of constant CO_2 mole fraction in saturated phase. See caption of Fig. 15.

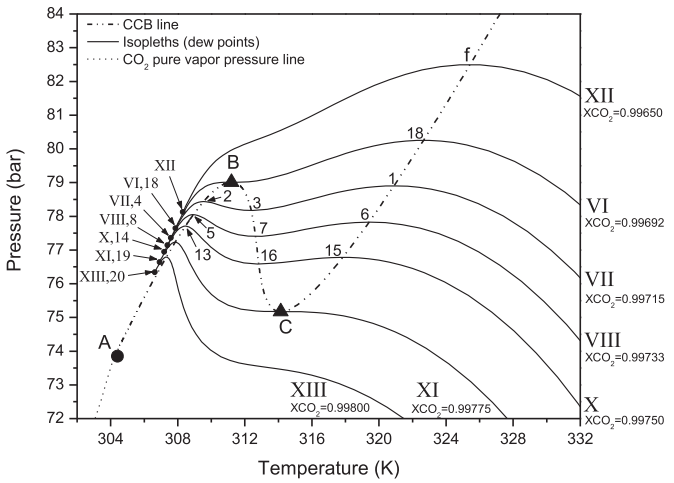

Fig. 18. Pressure–Temperature projection of calculated CCB line and calculated set of isopleths. CO_2 + n-decane system (RBxP and DRBxP). Full circles: critical points. Arabic and roman numbers are consistent with those of Figs. 16 and 17.

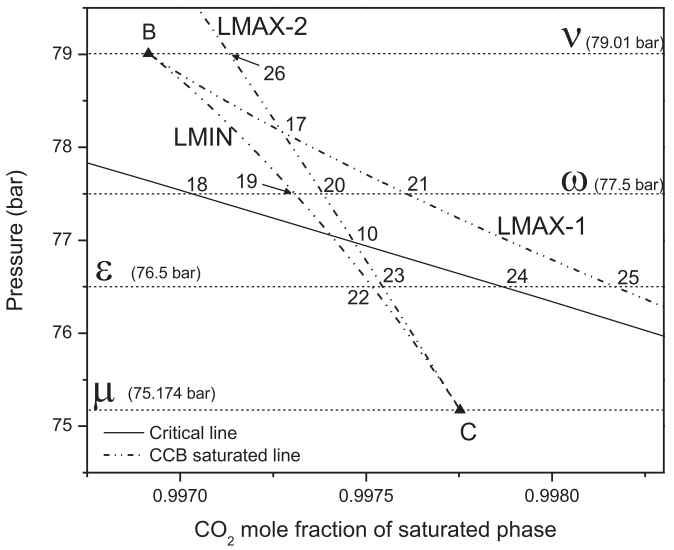

Fig. 19. Calculated CCB diagram. CO_2 + n-decane system. Horizontal dotted lines: constant pressure cuts. See caption of Fig. 15.

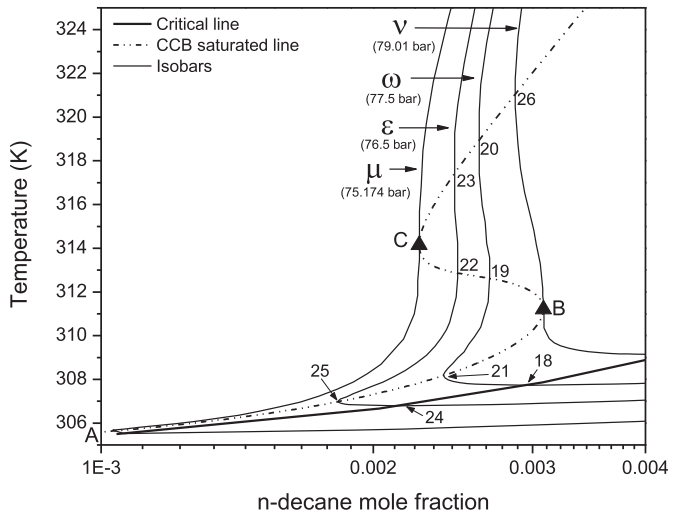

Fig. 20. Temperature – n-decane mole fraction in saturated phase projection of calculated CCB line and set of calculated isobars. The calculated critical line is also shown. System: CO_2 + n-decane (RBxP and DRBxP). See caption of Fig. 15.

the LMAX-2 line, the LMAX-1 branch of the CCB line (Fig. 16) is also a locus of isopleth (local or absolute) maxima in pressure (Fig. 18, CCB line from point A to point B). Finally, the LMIN branch of the CCB line in Fig. 16 is a locus of isopleth local minima in pressure (Fig. 18, CCB line from point B to point C). Point B is an inflection point of a specific isopleth (isopleth VI, Fig. 18). This is also the case for point C (isopleth XI, Fig. 18).

Fig. 17 is a zoom of Fig. 16. Isopleths VII, VIII, IX and X intersect all three branches of the CCB line. Hence, these isopleths have two local maxima and a single local minimum in pressure (Fig. 18).

As it can be seen in Fig. 16, isopleth VI intersects the CCB line at two points. One of them is point B, which is an inflection point of isopleth VI (Fig. 18). At point B, a local maximum and a local minimum in pressure merge into a single stationary point (Fig. 18). At point B, both, the first and second derivatives of pressure with respect to temperature are simultaneously equal to zero. At this point DRBxP is incipient. At a CO_2 mole fraction less than that of point B, only RBxP will be present in a given isopleth (e.g., isopleth XII in Fig. 18).

Similarly to isopleth VI, isopleth XI also intersects the CCB line at two points (Figs. 16 and 17). One of them is point C, the inflection point shown in Fig. 18 for isopleth XI. At isopleth CO_2 mole fraction values greater than that of point C in Fig. 17, only RBxP will be present (single intersection point).

Since (Fig. 17) point B is the intersection point of the LMAX-1 and LMIN branches, two local extrema of different kinds merge at point B (as previously stated in the context of Fig. 18). This is only possible if the slope is zero at point B for the pressure as a function of temperature, indeed for the isopleth with the composition of point B. Similar remarks can be made for point C. The isopleth composition range where DRBxP is potentially present is from point B composition to point C composition (Fig. 17).

We now go back to Fig. 11. Notice that if the pressure of point 2 (P2) were less than the pressure of the critical point (PCP), then, there would still be DRBxP, which would happen in the range PCP to P1. If P2 and P3 were both less than PCP, then, there would not be DRBxP. Thus, the condition for DRBxP, at set isopleth composition, is the existence of two local maxima in pressure with pressure values greater than that of the binary critical pressure. Both, isopleths VIII and IX meet this requirement (Fig. 17), in spite of the fact that three local extrema (points 5, 6 and 7) have all pressure values greater than that of the critical pressure (point 8) in isopleth VIII (Figs. 17 and 18), while, for isopleth IX (Fig. 17), the pressure of the local minimum (point 12) is less than the critical pressure (point 11). On the other hand, isopleth X (Fig. 17) has two local extrema in pressure (points 15 and 16) with pressures less than the critical pressure (point 14). Thus, isopleth X does not show DRBxP (Fig. 18).

Isopleth VII (Fig. 17), meets the above criterion for the existence of DRBxP (Fig. 18, curve VII). In this case, the pressure range where DRBxP occurs is from P_3 to P_2 (Figs. 17 and 18). Schematically, isopleth VII behaves as the isopleth in Fig. 11. Notice, in Fig. 17, that point 2 of isopleth VII belongs to the LMAX-1 branch. Isopleth VIII (Figs. 17 and 18) shows DRBxP in the pressure range from P_7 (LMIN branch) to P_6 (LMAX-2 branch). Thus, with regard to the range of existence of DRBxP, there is an exchange of branches when going from the lowest pressure local maximum point 2 (LMAX-1 branch, Fig. 17) in isopleth VII, to the lowest pressure local maximum point 6 (LMAX-2 branch, Fig. 17) in isopleth VIII.

Point 17 in Fig. 17 is the intersection point between branches LMAX-1 and LMAX-2. The isopleth of point 17, shows DRBxP with

Please cite this article in press as: J.I. Ramello, et al., Direct detection of double retrograde behavior in binary systems for equation of state models, Fluid Phase Equilibria (2016), http://dx.doi.org/10.1016/j.fluid.2016.02.044

both local maxima having the same pressure value (P_{17}). Point 17 is the one at which the exchange of LMAX branches takes place.

As previously stated, isopleth X does not show DRBxP (Figs. 17 and 18). However, it does show simple RBxP. Cleary, this isopleth corresponds to the schematic diagram of Fig. 13. At a pressure P^{*} in between P_{16} and P_{15} in Fig. 17, which correspond respectively, in Fig. 13, to points 2 and 1, an isobaric isoplethic decreasing temperature path (C, D, G in Fig. 13) has the evolution: V→V + L→V→V + L→L, where only the second step (V + L→V) is retrograde (RBxP). At P^{**} in between P_{14} and P_{13} in Fig. 17 (corresponding to points CP and 3 in Fig. 13) isopleth X also shows RBxP.

4.1.2. Analysis of vapor–liquid equilibrium isobars (RBxP, DRBxP)

The same analysis done for vapor–liquid isopleths can be done for vapor–liquid isobars. To begin, it can be seen in Fig. 20 how the CCB line connects all local extrema in mole fraction of a set of vapor–liquid isobars. Next, we see in Fig. 16 that a constant pressure section at 81 bar (χ horizontal line) intersects the CCB line at a single point. Thus, the isobar shows a unique local extremum in composition, i.e., a local maximum in x_{CO2} (point 1 in Fig. 9). Therefore, the χ isobar exhibits RBxP. From this, a given isobar of pressure greater than that of point B in Fig. 16, or in the pressure range from point A (pure CO_2 critical point) to point C (75.17 bar) (Fig. 16), has a single local maximum in x_{CO2} (RBxP).

Fig. 19 is a zoom of Fig. 16. Isobar ω has three local extrema in x_{CO2} (points 19, 20 and 21 in Fig. 19). All of them fall to the right of the critical point (point 18). Hence, the isobar will be as the one schematically shown in Fig. 12, and it will thus show DRBxP. This will happen in the composition range set by points 19 and 20 in Fig. 19. Isobar ω is quantitatively shown in Fig. 20. Points CP, 4, 5 and 6 in Fig. 12 respectively correspond to points 18, 20, 19 and 21 in Fig. 19. Notice that in Fig. 20 the abscissa is the mole fraction of the least volatile component (n-decane) (xC10), while in Fig. 12 the abscissa is the mole fraction of the most volatile component (x1).

In Fig. 20, a given local extremum in mole fraction (CCC_P point) has certain temperature (T_{CCCP}), pressure (P_{CCCP}) and n-decane mole fraction ($y_{C10\text{-}CCCP}$). Besides, the phase of composition $y_{C10\text{-}CCCP}$ is at equilibrium with another phase of composition $x_{C10\text{-}CCCP}$. Composition $y_{C10\text{-}CCCP}$ is equal to the composition of the saturated phase of an isopleth having a CCB point at conditions identical to those of the CCC_P point (T_{CCCP}, P_{CCCP} and $x_{C10\text{-}CCCP}$). For a given isobar in Fig. 20, the branch below the critical line is the one that reports, at higher pressures, the $x_{C10\text{-}CCCP}$ values.

Isobar ε in Fig. 19, as it happens for isobar ω, has also three local extrema in x_{CO2} (points 22, 23 and 25). However two of them (points 22 and 23) have x_{CO2} values that are less than the critical x_{CO2} (point 24). This is the situation in the schematic diagram of Fig. 14. Hence, isobar ε has only RBxP. It does in two different composition ranges, as illustrated in Fig. 14 (in this figure the path D to G is not retrograde). Points CP, 4, 5 and 6 in Fig. 14 correspond, respectively, to points 24, 25, 22 and 23. The calculated isobar ω is shown in Fig. 20.

Although it is not easily seen in Fig. 19, at about 77 bar there is a pressure range where, for a given isobar, only the local minimum in x_{CO2} has a x_{CO2} value less than the critical x_{CO2} value. The local maxima both exceed the critical x_{CO2} value. Such isobar would look as that of Fig. 12, except that point 5 in Fig. 12 would be shifted to a x_1 value less than that of point CP. In such a case we still have DRBxP.

The isobar of point 10 in Fig. 19, delimits the range of isobar pressure where DRBxP occurs, i.e., from the isobar pressure of point 10 to the isobar pressure of point B. In such range, the necessary condition of DRBxP is met, i.e., at least two CCC_P points have CO_2 mole fraction values greater than that of the critical point of the isobar. In Fig. 19, isobar μ (P = 75.174 bar) is the isobar of point C. At the pressure of point C, the presence of three local extrema in x_{CO2} is incipient. Point C is an inflection point of the isobar μ, as shown in Fig. 20.

4.2. Results on retrograde behavior at constant composition and temperature (RBxT, DRBxT)

4.2.1. Analysis of vapor–liquid equilibrium isopleths (RBxT, DRBxT)

Fig. 21 shows a convenient projection of the calculated CCT hyper-line, for system CO_2 + n-decane, in the CO_2-rich region: it is the temperature versus saturated phase CO_2 mole fraction projection. This diagram is helpful in identifying, for a given model, the ranges of conditions where DRBxT occurs. The number of intersection points (Fig. 21), between the CCT line and a given constant composition section (or constant temperature section), equals the number of isopleth CCT points (or the number of isotherm CCC_T points). For instance, from Fig. 21, the 0.99825 CO_2 mole fraction vapor–liquid equilibrium isopleth has a single CCT point at 341 K. Conversely, the 341 K vapor–liquid equilibrium isotherm has a CCC_T point at 0.99825 CO_2 mole fraction.

Point A in Fig. 21 is the pure CO_2 critical point. The cusp points B′ and C′ are not cusps in the multidimensional space of the CCT line. These points are local extrema of the CCT line (Fig. 21) and they are also inflection points of a couple of vapor–liquid isotherms (Fig. 26a) and of a couple of vapor–liquid isopleths (Fig. 25a).

Fig. 22 again shows the CCT line, but together with a number of isopleth and isotherm sections (vertical and horizontal lines, respectively).

Isopleth I (x_{CO2} = 0.9982, Fig. 22) intersects the LMAX-2 branch of the CCT line at a single point (point d). This point is a local maximum in temperature for isopleth I (point d in Fig. 25a, analogous to point 1 in Fig. 1). Consequently, the LMAX-2 branch is a locus of isopleth local maxima in temperature (see Fig. 25a). Branch LMAX-1 is also a locus of isopleth local maxima in temperature. Isopleth I in Fig. 22 exhibits RBxT, given that it has a single maximum in temperature (Figs. 1, 22 and 25a). All isopleths of CO_2 mole fraction less than that of point B′, or greater than the one of point C′, have a single CCT point, of the local maximum in temperature type. Branch LMIN is a locus of isopleth local minima in temperature.

The isopleth in Fig. 4 presents DRBxT. This isopleth has two local

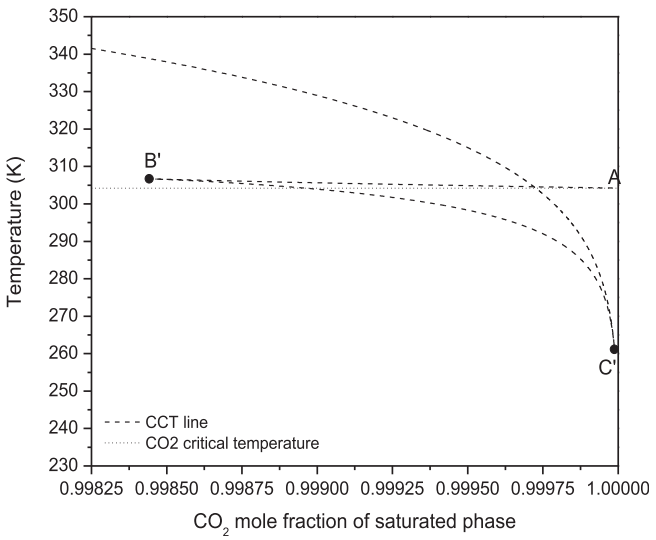

Fig. 21. CCT diagram. Temperature-CO_2 mole fraction in saturated phase projection of calculated CCT line. CO_2 + n-decane system. See caption of Fig. 15.

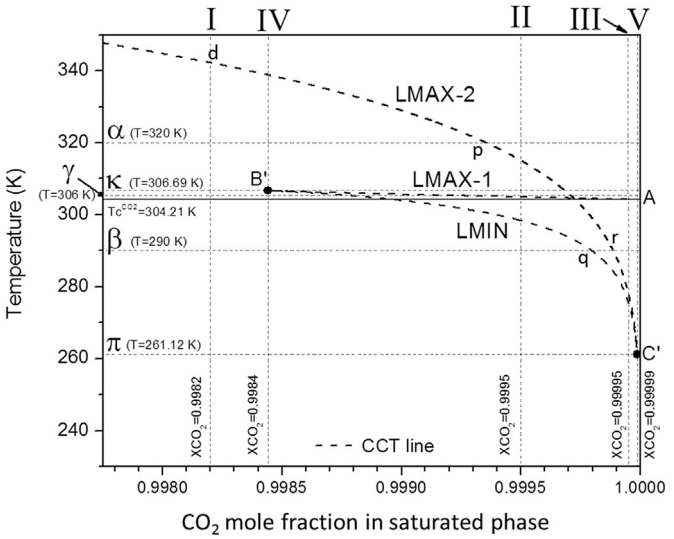

Fig. 22. Calculated CCT diagram. CO_2 + n-decane system. Horizontal dotted lines: constant temperature cuts. Vertical dotted lines: cuts of constant CO_2 mole fraction in saturated phase. See caption of Fig. 15.

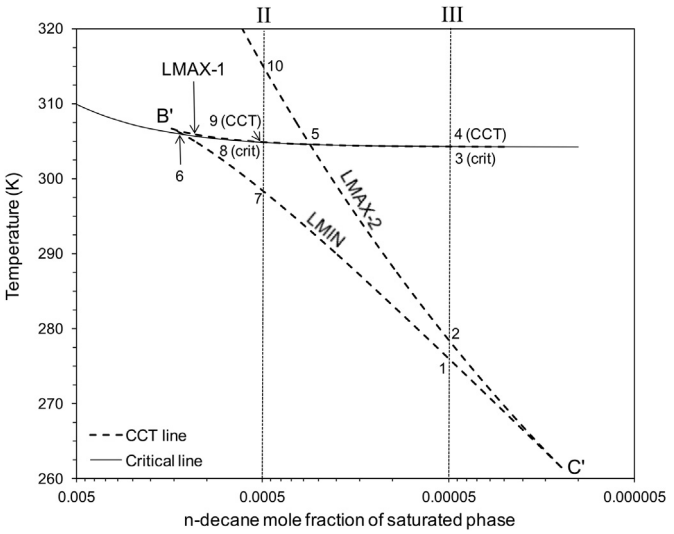

Fig. 23. Calculated CCT diagram. CO_2 + n-decane system. Vertical dashed lines: cuts of constant n-decane mole fraction in saturated phase. See caption of Fig. 15. Point B′: local maximum in temperature and local maximum in n-decane mole fraction in saturated phase. Point C′: local minimum in temperature and local minimum in n-decane mole fraction in saturated phase.

maxima in temperature (points 1 and 3) which have temperatures (T1 and T3) greater than that of the critical point (TCP). The DRBxT temperature range is the one indicated by lines I (TCP) and II (T1) in Fig. 4. T2 in Fig. 4 is less than TCP. If T2 were greater than TCP, then, there would still be DRBxT, but now in the temperature range from T2 to T1. In Fig. 6, T3 is less than TCP and no DRBxT is observed. However, simple RBxT is observed at two different temperature ranges in Fig. 6. In conclusion DRBxT is observed when two local maxima in temperature have temperatures greater than the mixture critical temperature.

Fig. 23 is a zoom of Fig. 22. Notice that in Fig. 23 (and in its zoom, i.e., Fig. 24) the composition variable (abscissa) is the n-decane mole fraction in the saturated phase, and that this variable increases from right to left (in Figs. 23 and 24), which is not the

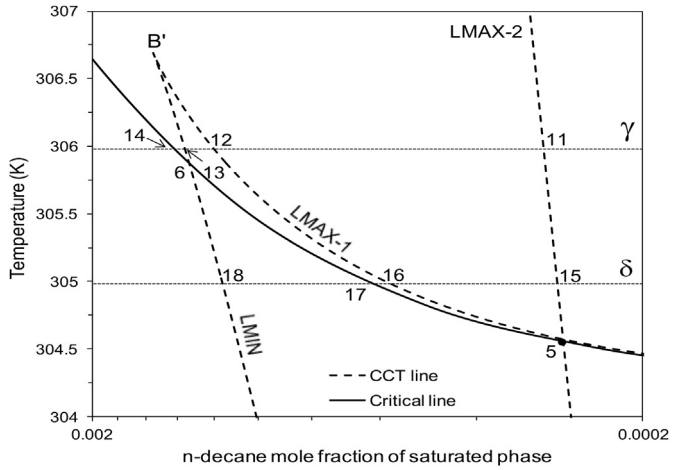

Fig. 24. Calculated CCT diagram. CO_2 + n-decane system. Horizontal lines: constant temperature cuts. See caption of Fig. 15.

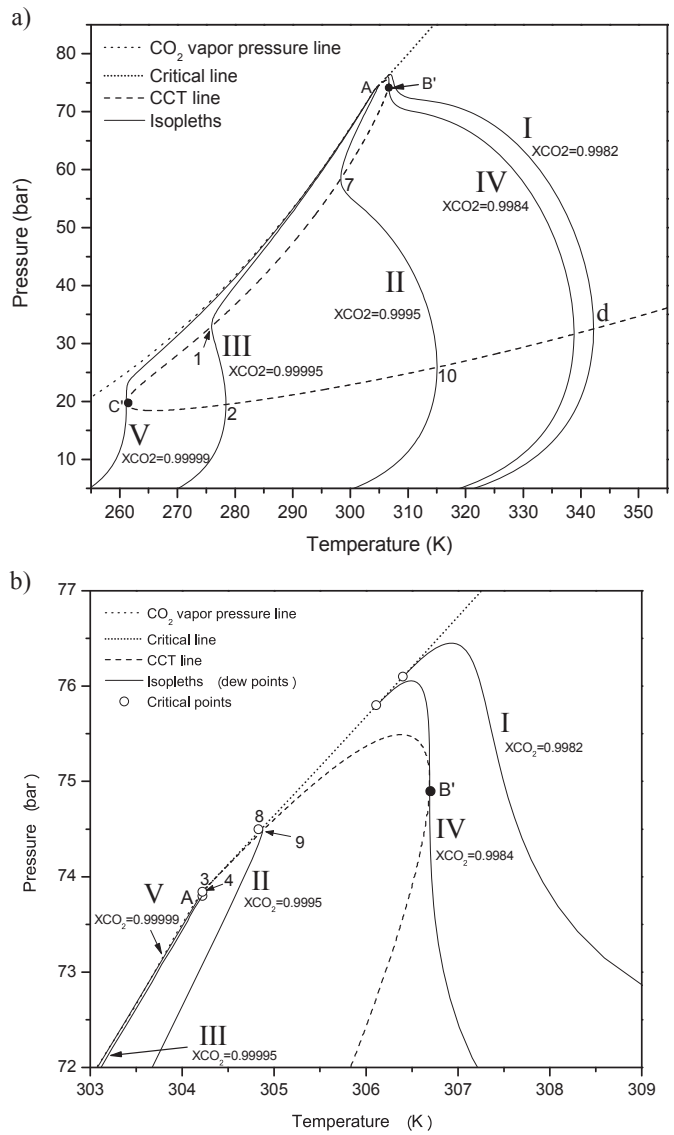

Fig. 25. Pressure–Temperature projection of calculated CCT line and set of calculated isopleths. CO_2 + n-decane system (RBxT and DRBxT). See caption of Fig. 15.

Please cite this article in press as: J.I. Ramello, et al., Direct detection of double retrograde behavior in binary systems for equation of state models, Fluid Phase Equilibria (2016), http://dx.doi.org/10.1016/j.fluid.2016.02.044

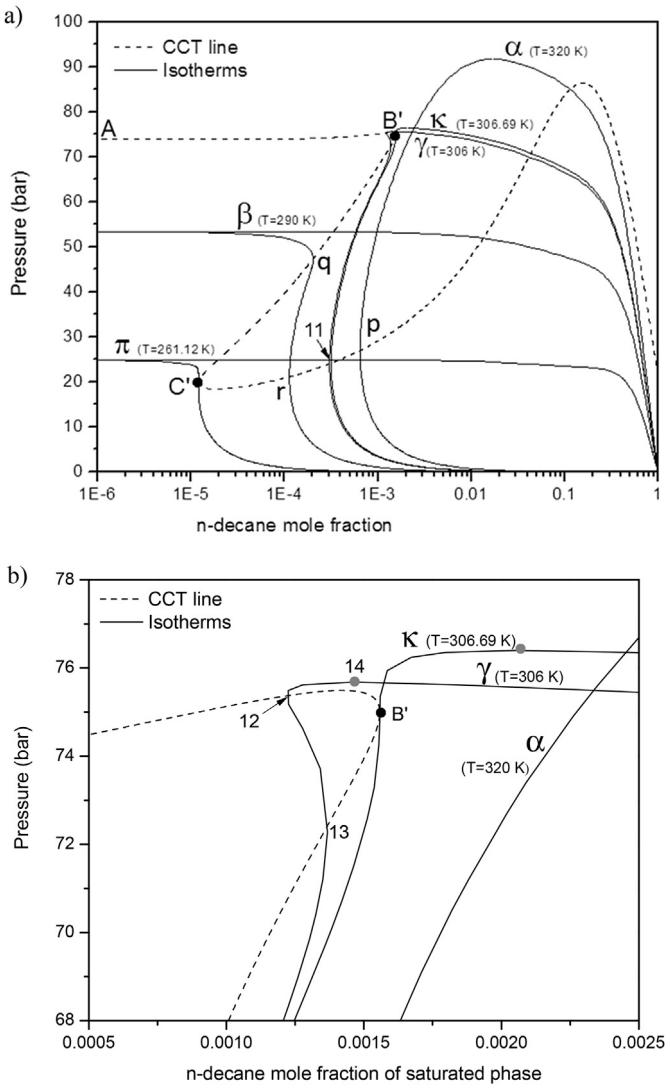

Fig. 26. Pressure - n-decane mole fraction in saturated phase projection of calculated CCT line, and set of calculated iotherms. CO_2 + n-decane system (sub-critical RBxT and DRBxT). See caption of Fig. 15.

typical convention for Cartesian diagrams. This unconventional increase in the abscissa makes possible to avoid confusion (i.e., to avoid the "mirror effect") when comparing Fig. 23 (and Fig. 24) with Fig. 22. Figs. 23 and 22 show that Isopleth II intersects the CCT line at three points (points 7, 9 and 10 in Fig. 23) and the critical line at point 8. In order of increasing temperature, these points follow the sequence: $T_7 < T_{8(crit)} < T_{9(CCT)} < T_{10}$.

Thus, since the two local maxima have a temperature greater than the critical temperature, isopleth II has DRBxT, which occurs in a narrow temperature range, i.e., from $T_{8(crit)}$ to T_9, as it is shown in Fig. 25a and b.

Isopleth III (Fig. 23) intersects the CCT line at points 1, 2 and 4 and the critical line at point 3. The temperature of the local maximum 2 (T_2) is less than the critical temperature ($T_{3(crit)}$). Thus, isopleth III does not exhibit DRBxT but simple RBxT, as shown schematically in Fig. 6 and quantitatively in Fig. 25a and b.

Isopleth IV (Fig. 22) intersects the CCT line at two points. One of them is point B′ at which the DRBxT is incipient. Point B′ is an inflection point in isopleth IV (Fig. 25a). Analogous statements apply to point C' (Figs. 22 and 23) and its associated isopleth, i.e., isopleth V (Figs. 22 and 25).

Fig. 24 is a zoom of Fig. 23. Fig. 24 clearly shows that the critical line is located below the LMAX-1 branch. We name z_5 the n-decane mole fraction at point 5 in Figs. 23 and 24. Point 5 is the intersection point between branches LMAX-1 and LMAX-2. Isopleths in the composition range from z_5 to $z_{B'}$ exhibit DRBxT, e.g., isopleth II (Figs. 23 and 25, Fig. 4), while those in the range from $z_{C'}$ to z_5 show no DRBxT but RBxT, e.g. isopleth III (Figs. 23 and 25, Fig. 6).

4.2.2. Analysis of vapor–liquid equilibrium isotherms (RBxT, DRBxT)

With regard to constant temperature sections, Fig. 5 shows a schematic isotherm with DRBxT. In such particular case all local extrema are located to the right of the critical composition. There would also be DRBxT if point 3 were located to the left of the critical composition as long as points 2 and 4 remain on the right.

In Fig. 22 isotherm π (261.12 K, horizontal line) contains point C′, i.e., the inflection point seen in Fig. 26a for isotherm π. 261.12 K is less than the CO_2 critical temperature (T_C = 304.21 K). At temperatures less than that of point C' (261.12 K), isothermal sections do not have RBxT because of the lack of local extrema in mole fraction.

In Fig. 22, isotherm α (T = 320 K) intersects the CCT line at a single point (point p), which is the single local extremum in mole fraction shown in Fig. 26a (point p) for curve α.

Because of the two intersections with the CCT line for isotherm β (T = 290 K) in Fig. 22 (points q and r), two local extrema in composition appear in Fig. 26a for isotherm β, which shows RBxT.

Isotherm γ (T = 306 K, Figs. 24 and 22) intersects the CCT line at points 11, 12 and 13 (Fig. 24). All of them are located to the right of the critical (point 14) line in Fig. 24. Thus DRBxT is present. One of the intersection points is the local extremum point 11 seen in Fig. 26a. The other two local extrema are more clearly seen in Fig. 26b (points 12 and 13, γ curve).

Isotherm δ in Fig. 24 intersects the CCT line at points 15, 16 and 18, and the critical line at point 17. Thus, isotherm δ exhibits DRBxT.

Isotherm κ (T = 306.69 K, Fig. 22), intersects the CCT line twice. One of the intersection points is point B′, i.e., the inflection point in curve κ of Fig. 26b. The other intersection point is the local extremum in mole fraction in curve κ of Fig. 26a. Isotherm κ is the one with highest temperature (T = $T_{B'}$) at which DRB is observed. At higher temperatures only RB will be present (e.,g., isotherm α, see Fig. 26a and b). Isotherm κ temperature is greater than the critical temperature of pure CO_2 (T = 304.21 K).

At point 5 in Fig. 23 (and Fig. 24) lines LMAX-2 and LMAX-1 intersect each other, as previously stated. The isotherm of Point 5 is the one with lowest temperature at which DRB is observed. In conclusion, DRBxT is observed for isothermal section temperatures in the range [T_5,$T_{B'}$]. In this range, a couple of local extrema of the same kind (L-MAX) are located to the same side of the critical line (Fig. 24). This is not the case for the temperature range [$T_{crit,pure\ CO2}$, T_5] where only RBxT is present ($T_{crit,pure\ CO2}$ is the temperature of point A in Fig. 22). This happens at two different ranges of composition (Fig. 7). Although it is not shown in the figures, the calculated binary critical line originates at the pure CO_2 critical point.

Finally, in the temperature range [$T_{C'}$, $T_{crit,pure\ CO2}$] (Fig. 22) RBxT will be observed for any isothermal section (e,.g., isotherm β in Fig. 26a), because of the intersections with the LMIN and LMAX-2 lines, at the set temperature (subcritical with respect to $T_{crit,pure\ CO2}$).

4.3. Example of a system without double retrograde behavior

Appendix A presents a number of figures for the case of a binary system not showing double retrograde behavior. Indeed, such system behaves in a simpler way than the CO_2 + n-decane system.

Please cite this article in press as: J.I. Ramello, et al., Direct detection of double retrograde behavior in binary systems for equation of state models, Fluid Phase Equilibria (2016), http://dx.doi.org/10.1016/j.fluid.2016.02.044

4.4. Step by step summary for the detection of DRB

To fix ideas, we provide in this section a step by step practical recipe to establish whether an EoS predicts the occurrence of DRB. We only address in this section the *DRBxP* case. The *DRBxT* case has a step by step procedure analogous to the one for the *DRBxP* case. The basic algorithm for the study of the *DRBxP* is the following:

1. Compute the binary critical line
2. Compute the CCB line
3. Plot (Plot A) the pressure versus x_1 projection of the CCB line (PxCCB-line, x_1 = mole fraction of lightest component) together with the pressure versus x_1 projection of the binary critical line.
4. For studying a vapor–liquid equilibrium isopleth of composition z_1:
   a. Add to Plot A a vertical line at composition z_1 (z_1-line)
   b. Find the intersection point between the z_1-line and the critical line: point [z1, P_{crit}(z1)]
   c. Find the intersection points between the z_1-line and the PxCCB-line. Record the pressure values and the number of intersection points (NIP).
      i. If NIP = 1 there is no DRBxP
      ii. If NIP = 3 there is potential DRB (Pressures: P_LMAX_1, P_LMAX_2, P_LMIN)
         ➢ If the set { P_LMAX_1, P_LMAX_2, P_LMIN } has two pressure values greater than P_{crit}(z1), then, there is DRBxP observable in the P-T projection of the isopleth of composition z_1). Otherwise there is no DRBxP
5. For studying a vapor–liquid equilibrium isobar of pressure P
   a. Add to Plot A an horizontal line at pressure P (P-line)
   b. Find the intersection point between the P-line and the critical line: point [x_{1crit}(P), P]
   c. Find the intersection points between the P-line and the PxCCB-line. Record the composition values and the number of intersection points (NIP).
      i. If NIP = 1 there is not DRBxP
      ii. If NIP = 3 there is potential DRB (mole fractions: z1_LMAX_1, z1_LMAX_2, z1_LMIN)
         ➢ If the set { z1_LMAX_1, z1_LMAX_2, z1_LMIN } has 2 mol fraction values greater than x_{1crit}(P), then, there is DRBxP observable in the T-x1 projection of the isobar of pressure P. Otherwise there is no DRBxP

We consider the described algorithm to be a straightforward one. Notice that step 4 can be applied to a range of z_1 values, and step 5 to a range of pressure values.

As stated above, the *DRBxT* case has a procedure analogous to that of the *DRBxP* case. The main differences are that, now, it is the CCT line the one to be plotted together with the critical line, and that their temperature versus x_1 projections are the ones to be studied.

5. Conclusions

In this work, a method to determine the ranges of conditions where (vapor–liquid equilibrium, VLE) double retrograde behavior (DRB) is present, for a given binary system, as represented by an equation of state (EoS) model, is proposed. The application of the new method is illustrated for the case of carbon dioxide + n-decane modeled by the RKPR EoS coupled to cubic mixing rules (CMRs). The method is based on the computation of cricondenbar (CCB) and cricondentherm (CCT) lines (each one in a single run) which are combined with computed critical lines to study the DRB. Plots of computed binary CCB (Fig. 16) and CCT (Fig. 21) lines, also including computed critical lines, make possible to evaluate, at a glance, whether the DRB is present. In this way, the computation of several VLE isopleths (or of several isobars or isotherms) is avoided. The high non linearity of the CCB and CCT lines is dealt with by using a numerical continuation method.

The case where a CCB or CCT line ends due to the instability of the liquid phase (liquid–liquid–vapor equilibrium) was not considered in this work. This will be the matter of future work.

Acknowledgments

We are grateful, for their financial support, to Consejo Nacional de Investigaciones Científicas y Técnicas de la República Argentina (CONICET), Universidad Nacional del Sur (U.N.S., Arg.), Universidad Nacional de Córdoba (U.N.C., Arg.) and Agencia Nacional de Promoción Científica y Tecnológica (ANPCyT, Arg.).

Appendix A. A system without double retrograde behavior

This appendix presents calculation results for the system propane + n-octane, as represented by the model indicated in the caption of Fig. A-1.

Fig. A-1 presents in the P vs T plane the calculated critical and CCB lines, and calculated phase envelopes at three different saturated phase propane mole fraction values. Points 1 and 2 are isopleth CCB points: both points belong to the CCB line. Points 3 and 4 are isopleth critical points which indeed belong to the critical line. Point A is simultaneously a CCB point and a critical point: the CCB and critical lines meet at point A.

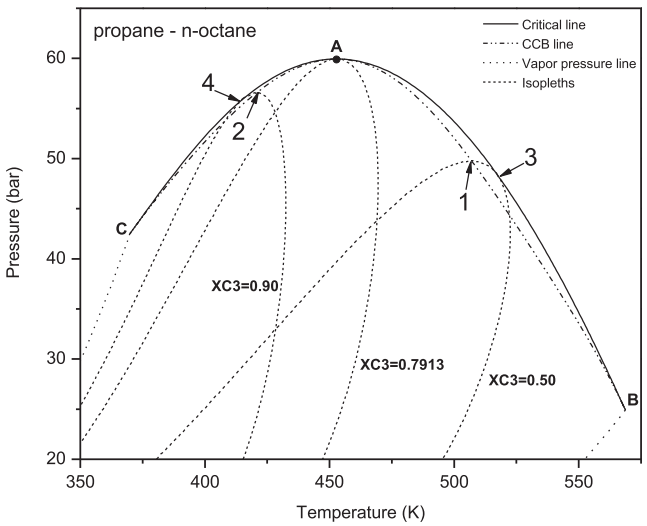

Fig. A-1. Calculated Pressure–Temperature projections of CCB, critical and pure compound vapor pressure lines, and calculated set of isopleths. Propane + n-octane system (Type I in Scott and van Konynenburg classification [25,26]). Point B: Critical point of pure n-octane. Point C: Critical point of pure propane. All lines were calculated using the RK-PR EoS and quadratic mixing rules with parameters k_{12} = 0.01443 and l_{12} = −0.03298 obtained from Ref. [27]. XC3: isopleth propane mole fraction.

Fig A-2 shows the projection Pressure vs. saturated phase propane mole fraction for the calculated critical and CCB lines. Since a vertical line at any set composition (isopleth) intersects the CCB line only once, this binary system shows no DRBxP. The same conclusion is reached by considering horizontal lines at any set pressure value (isobar).

Please cite this article in press as: J.I. Ramello, et al., Direct detection of double retrograde behavior in binary systems for equation of state models, Fluid Phase Equilibria (2016), http://dx.doi.org/10.1016/j.fluid.2016.02.044

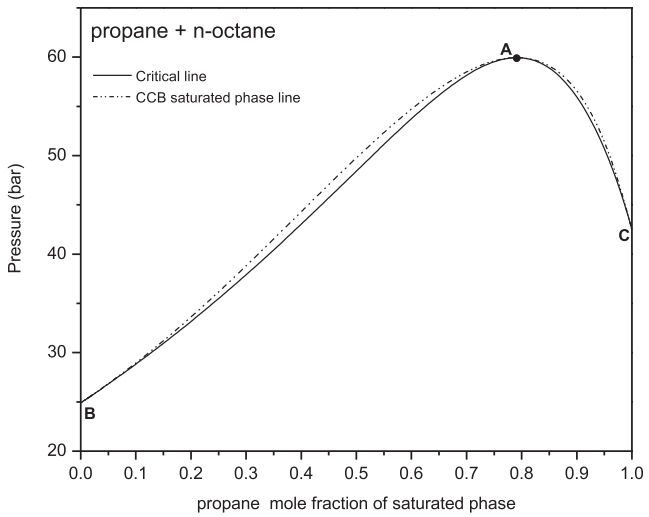

Fig. A-2. Calculated Pressure–propane mole fraction in saturated phase projections of CCB and critical lines. Propane + n-octane system. See caption of Fig. A-1.

Fig. A-3 is analogous to Fig. A-1. It presents the CCT line instead of the CCB line. Points 1, 2 and 3 are isopleth CCT points interconnected by the CCT line. Points D, E and F are spurious (only apparent) intersection points between the CCT line and the isopleths.

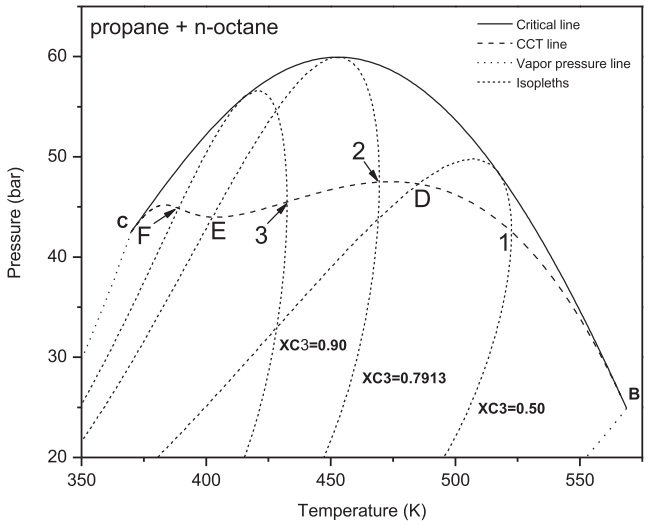

Fig. A-3. Calculated Pressure–Temperature projections of CCT, critical and pure compound vapor pressure lines, and calculated set of isopleths. See caption of Fig. A-1.

Fig. A-4 shows the calculated Temperature – propane mole fraction in saturated phase projections of CCT and critical lines. Vertical lines at constant composition (isopleth) would lead to the conclusion of absence of DRBxT due to existence of just a single intersection point between the vertical and CCT lines. The same conclusion would be obtained by considering horizontal lines at constant temperature (isotherms).

In conclusion, none of the two DRB types (DRBxP, DRBxT) is presented by the propane + n-octane system, which therefore behaves in a much simpler way than the CO_2 + n-decane system, considered in the main text of this paper.

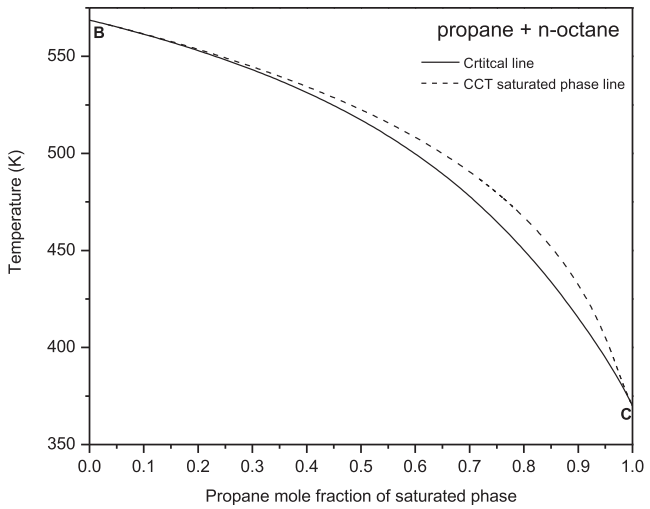

Fig. A-4. Calculated Temperature – propane mole fraction in saturated phase projections of CCT and critical lines. See caption of Fig. A-1.

References

[1] D.L. Katz, F. Kurata, Retrograde condensation, Ind. Eng. Chem. 32 (1940) 817–827, http://dx.doi.org/10.1021/ie50366a018.
[2] R.J.J. Chen, P.S. Chappelear, R. Kobayashi, Dew-point loci for methane-n-butane binary system, J. Chem. Eng. Data 19 (1974) 53–58.
[3] R.J.J. Chen, P.S. Chappelear, R. Kobayashi, Dew-point loci for methane-n-pentane binary system, J. Chem. Eng. Data 19 (1974) 58–61, http://dx.doi.org/10.1021/je60060a010.
[4] J.L. Bischoff, R.J. Rosenbauer, K.S. Pitzer, The system NaCl-H2O: Relations of vapor-liquid near the critical temperature of water and of vapor-liquid-halite from 300° to 500°C, Geochim. Cosmochim. Acta 50 (1986) 1437–1444.
[5] S. Raeissi, C.J. Peters, Phase behaviour of the binary system ethane+limonene, J. Supercrit. Fluids 22 (2002) 93–102. http://dx.doi.org/10.1016/S0896-8446(01)00118-8.
[6] S. Raeissi, C.J. Peters, On the phenomenon of double retrograde vaporization: multi-dew point behavior in the binary system ethane + limonene, Fluid Phase Equilib. 191 (2001) 33–40.
[7] S. Raeissi, C.J. Peters, Double retrograde vaporization in the binary system ethane + linalool, J. Supercrit. Fluids 23 (2002) 1–9.
[8] S. Raeissi, J.C. Asensi, C.J. Peters, Phase behavior of the binary system ethane+linalool, J. Supercrit. Fluids 24 (2002) 111–121. http://dx.doi.org/10.1016/S0896-8446(02)00035-9.
[9] S. Raeissi, C.J. Peters, Double retrograde vaporization in a multi-component system: ethane+orange peel oil, J. Supercrit. Fluids 29 (2004) 69–75. http://dx.doi.org/10.1016/S0896-8446(03)00068-8.
[10] M.F. Alfradique, M. Castier, Effect of combining rules for cubic equations of state on the prediction of double retrograde vaporization, Fluid Phase Equilib. 230 (2005) 1–8.
[11] U.K. Deiters, Some comments on the double retrograde vaporization, J. Chem. Thermodyn. 35 (2003) 583–589.
[12] S. Raeissi, C.J. Peters, Thermodynamic analysis of the phenomenon of double retrograde vaporization, J. Phys. Chem. B 108 (2004) 13771–13776.
[13] S. Raeissi, C.J. Peters, Simulation of double retrograde vaporization using the Peng-Robinson equation of state, J. Chem. Thermodyn. 35 (2003) 573–581.
[14] S. Espinosa, S. Raeissi, E.A. Brignole, C.J. Peters, Prediction of double retrograde vaporization: Transitions in binary mixtures of near critical fluids with components of homologous series, J. Supercrit. Fluids 32 (2004) 63–71.
[15] I. Wichterle, High pressure vapour-liquid equilibrium. I. Phenomenological description. Part 1, Fluid Phase Equilib. 1 (1977) 161–172.
[16] M.A. Barrufet, P.T. Eubank, New physical constraints for fluid mixture equations of state and mixture combining rules, Fluid Phase Equilibria 37 (0) (1987) 223–240.
[17] E.H. Chimowitz, Introduction to Critical Phenomena in Fluids, Oxford University Press, New York, 2005.
[18] M. Cismondi, M.L. Michelsen, Global phase equilibrium calculations: Critical lines, critical end points and liquid–liquid–vapour equilibrium in binary mixtures, J. Supercrit. Fluids 39 (2007) 287–295, http://dx.doi.org/10.1016/j.supflu.2006.03.011.
[19] M. Cismondi, M. Michelsen, Automated calculation of complete Pxy and Txy diagrams for binary systems, Fluid Phase Equilib. 259 (2007) 228–234.
[20] M. Cismondi, M.L. Michelsen, M.S. Zabaloy, Automated generation of phase diagrams for binary systems with azeotropic behavior, Ind. Eng. Chem. Res. 47 (2008) 9728–9743.
[21] S.B. Rodriguez-Reartes, M. Cismondi, M.S. Zabaloy, Computation of solid-fluid-fluid equilibria for binary asymmetric mixtures in wide ranges of conditions,

J. Supercrit. Fluids 57 (2011) 9–24.
[22] G. Pisoni, M. Cismondi, L. Cardozo-Filho, M.S. Zabaloy, Generation of characteristic maps of the fluid phase behavior of ternary systems, Fluid Phase Equilib. 362 (2014) 213–226, http://dx.doi.org/10.1016/j.fluid.2013.10.010.
[23] G. Pisoni, M. Cismondi, L. Cardozo-Filho, M.S. Zabaloy, Critical end line topologies for ternary systems, J. Supercrit. Fluids 89 (2014) 33–47, http://dx.doi.org/10.1016/j.supflu.2014.01.014.
[24] M. Cismondi, S.B. Rodríguez-Reartes, J.M. Milanesio, M.S. Zabaloy, Phase equilibria of CO 2 + n-alkane binary systems in wide ranges of conditions: Development of predictive correlations based on cubic mixing rules, Ind. Eng. Chem. Res. 51 (2012) 6232–6250.
[25] R.L. Scott, P.H. Van Konynenburg, Static properties of solutions: Van der Waals and related models for hydrocarbon mixtures, Discuss. Faraday Soc. 49 (1970) 87–97.
[26] R. Privat, J.-N. Jaubert, Classification of global fluid-phase equilibrium behaviors in binary systems, Chem. Eng. Res. Des. 91 (10) (2013) 1807–1839.
[27] J.M. Milanesio, R. Srivastava, J.C. Hassler, E. Kiran, Continuous Density Measurements and Volumetric Properties of Mixtures of Propane and n-Octane at High Pressures, in: 18th Symposium on Thermophysical Properties, Boulder, Colorado, 2012.

Please cite this article in press as: J.I. Ramello, et al., Direct detection of double retrograde behavior in binary systems for equation of state models, Fluid Phase Equilibria (2016), http://dx.doi.org/10.1016/j.fluid.2016.02.044